

Structure and clumping in the fast wind of NGC 6543

R. K. Prinja,^{1★} S. E. Hodges,^{1★} D. L. Massa,^{2★} A. W. Fullerton^{3★} and A. W. Burnley^{1★}

¹*Department of Physics & Astronomy, University College London, Gower Street, London WC1E 6BT*

²*SGT, Inc., NASA Goddard Space Flight Center, Code 681.0, Greenbelt, MD 20771, USA*

³*Space Telescope Science Institute, 3700 San Martin Drive, Baltimore, MD 21218, USA*

Accepted 2007 August 15. Received 2007 August 14; in original form 2007 July 3

ABSTRACT

Far-ultraviolet spectroscopy from the *FUSE* satellite is analysed to *uniquely* probe spatial structure and clumping in the fast wind of the central star of the H-rich planetary nebula NGC 6543 (HD 164963). Time-series data of the unsaturated P v $\lambda\lambda$ 1118, 1128 resonance line P Cygni profiles provide a very sensitive diagnostic of variable wind conditions in the outflow. We report on the discovery of episodic and recurrent optical depth enhancements in the P v absorption troughs, with some evidence for a ~ 0.17 -d modulation time-scale. Empirical line-synthesis modelling is used to derive physical properties, including the optical depth evolution of individual ‘events’. The characteristics of these features are essentially identical to the ‘discrete absorption components’ (DACs) commonly seen in the ultraviolet lines of massive OB stars. We have also employed the unified model atmosphere code CMFGEN to explore spectroscopic signatures of clumping, and report, in particular, on the clear sensitivity of the P v lines to the clump volume filling factor. The results presented here have implications for the downward revision of mass-loss rates in planetary nebula central stars. We conclude that the temporal structures seen in the P v lines of NGC 6543 likely have a physical origin that is similar to that operating in massive, luminous stars, and may be related to near-surface perturbations caused by stellar pulsation and/or magnetic fields.

Key words: stars: evolution – stars: individual: NGC 6543 – stars: winds, outflows.

1 INTRODUCTION

As the immediate precursors of white dwarfs, the central stars of planetary nebulae (CSPNs) provide fundamental tests in key areas of stellar astrophysics, including evolutionary theory, non-local thermodynamic equilibrium (non-LTE) model atmospheres and plasma hydrodynamics. An important challenge is to understand details of the mass-loss process through the planetary nebula stage. Specifically, the fast winds of CSPN provide a probe of the *current* mass loss, and represent a valuable setting for the study of radiative and mechanical interactions between stars and their environments.

Shortly after the launch of the *International Ultraviolet Explorer* (*IUE*) satellite, it became clear that fast winds are a common feature of CSPN (e.g. Heap 1979; Perinotto, Cerruti-Sola & Benvenuti 1982). The P Cygni ultraviolet (UV) resonance line profiles have been decoded to record maximum wind velocities of up to a few 1000 km s⁻¹ and estimates of the mass-loss rate range between $\sim 10^{-11}$ and $10^{-6} M_{\odot} \text{ yr}^{-1}$ (see e.g. Perinotto 1989, and references within). Our objective in this paper is to exploit new *Far-Ultraviolet*

Spectroscopic Explorer (*FUSE*) satellite time-series spectroscopy of the central star of NGC 6543 to uniquely examine the time-variable characteristics of its fast wind.

An improved understanding of variability and clumping in the fast winds of CSPN is important for several reasons: temporally variable spatial structure implies a clumped and at least locally non-spherical fast wind, which can modify how the supersonic outflow interacts with the nebular material (e.g. Falle et al. 2002; Steffen & Lopez 2003). Substantial wind clumping can also significantly complicate determinations of the mass-loss rates from the central stars. For example, recent analyses of optical and UV lines in luminous, massive O-type stars have provided evidence for extreme wind clumping factors, with implications that the mass-loss rates of OB stars may have previously been overestimated by factors of between 3 and 10 (e.g. Hillier, Lanz & Heap 2003; Massa et al. 2003; Markova et al. 2004; Bouret, Lanz & Hillier 2005; Fullerton, Massa & Prinja 2006).

Recent *Chandra* and *XMM-Newton* observations have established the presence of diffuse X-ray emission from *within* the nebular interior regions (e.g. Guerrero et al. 2001; Kastner et al. 2003; Maness & Vrtilik 2003). The source of the X-rays from the central star vicinity remains uncertain, and one possible origin would be the presence of shock-heated gas arising from instabilities in a variable fast wind (e.g. Akashi, Soker & Behar 2006).

*E-mail: rkp@star.ucl.ac.uk (RKP); seh@star.ucl.ac.uk (SEH); massa@taotaomona.gsfc.nasa.gov (DLM); fullerton@stsci.edu (AWF); awxb@star.ucl.ac.uk (AWB)

The present study is also motivated by a need to understand the relation between optical spectroscopic (radial velocity) and photometric changes evident in several CSPN. The frequently imaged non-spherical and bipolar morphologies of the planetary nebulae (e.g. Zuckerman & Aller 1986) raise the possibility that the planetary nebulae may have been ejected via common envelope interaction in close binary central stars (e.g. Sandquist et al. 1998). Surveys of the PN binary population are currently frustrated by the physical interpretation of the observed radial velocity and photometric variations, which might at least in part be due to changes in the fast wind (e.g. Handler 2003; De Marco et al. 2004).

There is a clear need therefore to investigate further the detailed temporal variability of the fast winds in CSPN. To date, studies of variability in these outflows have primarily relied on (limited) multiple UV spectra obtained with the *IUE* satellite (e.g. Patriarchi & Perinotto 1997). Generally, however, the detection of wind line variability with *IUE* (or *HST*) was extremely difficult since the only UV resonance lines accessible are strongly saturated, thus masking all changes except at the extreme violet edges of the line profiles. In addition, the exposure times of high-resolution *IUE* spectra were rather long, that is, ~ 2 to 3 h, which is in fact comparable to the wind flushing time in these stars. We provide here new perspectives on variability in the fast winds of CSPN by exploiting *FUSE* ($\lambda\lambda 905$ to 1187 \AA) time-series observations. *FUSE* can uniquely deliver the requisite high-signal-to-noise ratio data in short integration times, while also potentially providing access to *unsaturated* resonance lines, including P v, S iv, S vi, O vi and C iii.

1.1 The target, NGC 6543

We present in this paper, a study of structure and variability in the fast wind of the CSPN NGC 6543 (HD 164963; BD +66° 1066). The nebula is well studied, with *HST* images in particular revealing complex structures that include phenomena such as bubbles and precessing jets (e.g. Harrington & Borkowski 1994; Balick 2004; Wesson & Liu 2004). X-ray emission has been detected with *Chandra* (Chu et al. 2001; Guerrero et al. 2001), which is consistent with a point source at the central star and diffuse emission from within the elliptical central shell. Various studies have reported evidence for time-variable changes associated with the central star, including Mendez, Herrero & Manchado (1990, optical spectroscopy), Bell, Pollacco & Hilditch (1994, photometry), and Patriarchi & Perinotto (1997, UV spectroscopy). Fundamental parameters of the central star based on non-LTE model atmosphere analysis have been derived by de Koter et al. (1996, ISA-WIND code) and Georgiev et al. (2006, CMFGEN). Key adopted parameters for the central star in NGC 6543 are listed in Table 1. We note that for a ' $\beta = 1$ '-type wind velocity law (e.g. Section 5), the wind flushing time to travel from 0.1 to 0.9 of the terminal velocity (v_∞) is only ~ 45 min.

2 FUSE TIME-SERIES DATA

Our study of the fast wind of NGC 6543 is largely based on *FUSE* data from Program F034 (PI – DL Massa), secured between 2007 January 13 and 16. A summary log of observations is provided in Table 2. The observations were obtained through the medium resolution aperture (MDRS; $4 \times 20 \text{ arcsec}^2$) aperture, spanning a total wavelength range of $905\text{--}1187 \text{ \AA}$ at a spectral resolution of $\sim 15 \text{ km s}^{-1}$. (The instrument and performance is discussed by Moos et al. 2000 and Sahnou et al. 2000). Typical individual integration times in HIST mode are ~ 10 min. Using the MDRS aperture unfortunately meant that occasionally the target was not fully captured

Table 1. NGC 6543 central star parameters.

Parameter	Value	Reference
Spectroscopy type	Of-WR (H-rich)	Mendez et al. (1990)
Luminosity	$5200 L_\odot$	de Koter et al. (1996)
T_{eff}	63 000 K	Georgiev et al. (2006)
Radius	$0.6 R_\odot$	Georgiev et al. (2006)
Distance	$1001 \pm 269 \text{ pc}$	Reed et al. (1999)
Mass-loss rate	$\sim 1 \times 10^{-7} M_\odot \text{ yr}^{-1}$	de Koter et al. (1996); Georgiev et al. (2006)
Terminal velocity	1400 km s^{-1}	This study
Wind flushing time	45 min	This study

Table 2. Summary log of *FUSE* observations.

Observation ID	Number of exposures	UT Date	MJD (start)	ΔT (h)
F0340105	26	2007 January 13	54 113.1260	9.7
F0340106	18	2007 January 14	54 114.1097	5.9
F0340107	19	2007 January 15	54 115.0933	7.3
F0340108	9	2007 January 16	54 116.0680	1.4

and there were cases of light loss. The most usable components are 59 spectra (processed through CALFUSE version 3.1.8) in the LiF2 channel (segment A; $\lambda\lambda 1086$ to 1182 \AA) which covers the strategic line of P v $\lambda\lambda 1117.98, 1128.01$. A sparser sequence of 29 spectra for the LiF1 channel (segment A; $\lambda\lambda 987$ to 1082 \AA) provided some information on the behaviour of the (stronger) O vi $\lambda\lambda 1031.92, 1037.62$ wind-formed line.

The mean *FUSE* spectrum is shown in Fig. 1. Aside from P v and O vi, a strong P Cygni line is also seen in S vi $\lambda\lambda 933.38, 944.52$. There is some evidence for blueward absorption in the excited N iv $\lambda 955.34$ line profile and C iii $\lambda 1175.67$. The remainder of the spectrum is dominated by narrow interstellar and circumsystem absorption lines due to atomic species and molecular hydrogen.

Overall, the mean *FUSE* spectrum of the central star in NGC 6543 is very similar to that seen in archival data in 2001 October (Prog. Q108) and 2006 March (prog. F034). The spectrum in Fig. 1 also closely matches the *ORPHEUS* spectrum obtained in 1993 September by Zweigle et al. (1997). Note for completeness that the *IUE* high-resolution spectrum of NGC 6543 is dominated by saturated P Cygni profiles of C iv $\lambda\lambda 1548.20, 1550.77$ and N v $\lambda\lambda 1238.82, 1242.80$, plus well-developed blueward absorption in O v $\lambda 1371.29$ and the excited line of N iv $\lambda 1718.55$ (e.g. Patriarchi & Perinotto 1997).

3 VARIABILITY

The P v resonance doublet in NGC 6543 is a well developed but unsaturated P Cygni profile, and thus offers the primary diagnostic of variable fast wind conditions in our dataset. A pair of P v line profiles separated by ~ 2 d is shown in Fig. 2, to illustrate what is essentially the maximum extent of profile fluctuations evident. A correction for a heliocentric systemic velocity of -66 km s^{-1} (Schneider et al. 1983) was applied by subtracting this value. Mostly the flux changes are at ~ 10 to 20 per cent of the continuum level and occur over localized blueward velocity regions, as opposed to the flux increasing or decreasing simultaneously over the *entire* absorption trough. As is the case with massive OB stars, the P v P Cygni *emission* profiles in NGC 6543 are quite constant. The overall variance in the

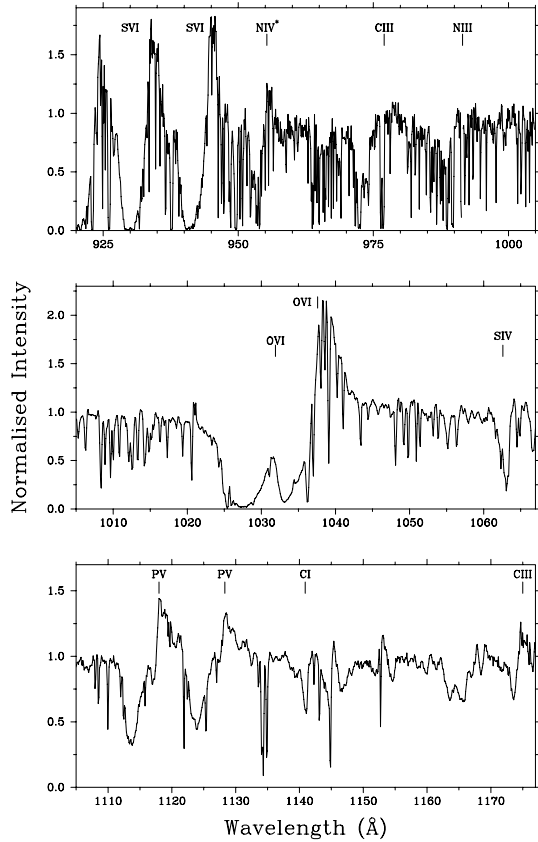


Figure 1. Mean *FUSE* spectrum of the central star in NGC 6543 from the F034 run in 2007 January.

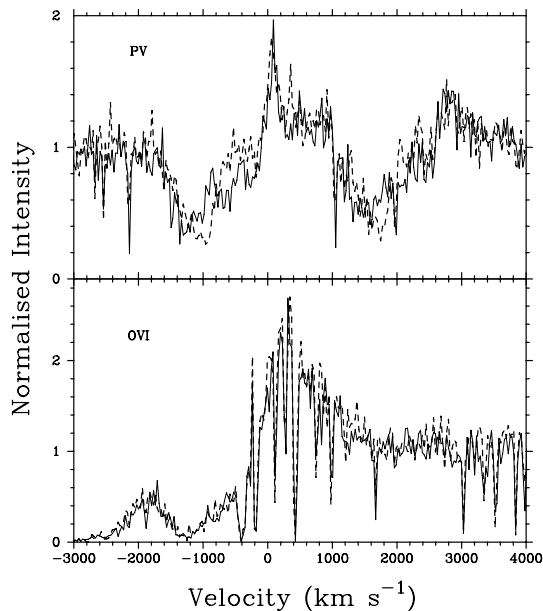


Figure 2. Fluctuations in the P *v* resonance line profiles compared to the more stable low-velocity regions of O *vi* λ 1037.6.

full 2007 time-series is certainly significant between ~ -500 and -1300 km s^{-1} . The equivalent width of the P *v* line is not conserved, and fluctuates between ~ 0.7 and 2.2 \AA (sd 0.3 \AA) for the blue component of the doublet (e.g. measured between 1111 and 1120 \AA).

Any changes in the other spectral lines are rather subtle if present at all. The lower panel in Fig. 2 shows the corresponding

line profiles of O *vi* λ 1037.62. Even the low-velocity (redward of ~ -600 km s^{-1}) region of this line is likely optically thick and variance analysis does not support any changes in O *vi* that are significant above a 95 per cent confidence level.

The data for P *v* are by contrast very revealing. Representations of the variability evident are displayed in Fig. 3 as dynamic spectra (i.e. two-dimensional images of individual spectra ordered in time). The images reveal clear evidence for systematic and organized line profiles changes. Specifically, localized (in velocity) absorption enhancements are seen (darker shades in Fig. 3) migrating blueward from ~ -400 to ~ -1000 km s^{-1} . We identify at least four separate episodes of recurring features. The patterns in Fig. 3 are essentially identical to the ‘discrete absorption components’ (DACs) commonly seen in UV resonance lines formed in the radiation-pressure-driven winds of massive OB stars (e.g. Kaper et al. 1996; Prinja, Massa & Fullerton 2002). The lower left-hand panels in Fig. 3 focus on three of the more prominent DAC-like features in NGC 6543, with central velocities that increase between ~ -830 and -1010 km s^{-1} over 1.1 h, ~ -510 and -1290 km s^{-1} over 6.0 h and ~ -700 and -1070 km s^{-1} over 1.3 h.

The DAC velocities above provide (linear) accelerations of between 3×10^{-2} and 8×10^{-2} km s^{-2} . These values for NGC 6543 are up to a factor of 10 faster than typical acceleration rates measured for features in OB star wind (e.g. Prinja 1998). However, the characteristic radial flow time of the wind (which scales as $\sim R_{\star}/v_{\infty}$) in NGC 6543 is only ~ 5 min (Table 1), compared to approximately hours for O stars. The time-scales associated with the DACs in NGC 6543 are therefore significantly greater than the wind flushing time over the line formation region, which suggests that it is very unlikely the wind structures in the PN central star are due to processes entirely intrinsic to the fast wind. The DACs cannot, for example, be due to mass-conserved shells or blobs ‘riding’ with the outflow from the star. As is widely believed for OB stars, the perturbations more likely arise as a result of inhomogeneities close to the stellar surface, such as pulsations or magnetic fields. The empirical evidence provided here suggests that the physical mechanism for initiating wind structure in the fast wind of NGC 6543 may be the same as that operating in massive, luminous stars (see Section 6).

4 MODULATED OR CYCLIC BEHAVIOUR

In a few case studies based on very extended *IUE* spectroscopy it has been demonstrated that the DACs in OB stars are modulated or quasi-cyclic, on variability time-scales that may relate to stellar rotation periods (e.g. Massa et al. 1995; Fullerton et al. 1997; de Jong et al. 2001; Prinja et al. 2002). From the viewpoint of nebular shapes, central star binarity and wind structure in line-driven winds, it is obviously interesting to consider whether the optical depth changes seen in the P *v* lines of NGC 6543 are systematically variable. The rotation period of NGC 6543 is not known, and determinations of the projected rotation velocities are sparse for PN central stars in general. Note also that the central star in our study is a member of the ZZ Lep class of variable stars (e.g. Handler 2003). Bell et al. (1994) document differences of ~ 0.01 mag in 5300 \AA CCD photometry though with little evidence for periodic variations that are consistent over the four nights of their observations. Individual nights provided evidence for modulations over ~ 2.6 and 3.2 h. Analysing the same dataset, Handler (2003) cites a photometric modulation of 3.5 ± 1.5 h. The origin of the photometric changes in NGC 6543 may relate to photospheric (pulsational) changes or indeed the inner regions of the fast wind. The strong FUV photospheric lines in our *FUSE* data

are relatively fixed in velocity (to within $\pm 10 \text{ km s}^{-1}$) and do not support any significant role for binary motion.

A periodogram analysis was carried out to search for evidence of repetitive or cyclic properties in the P v line profile changes. The basic Fourier method involved uses the iterative CLEAN algorithm (Roberts, Lehár & Dreher 1987) to deconvolve the features of the

window function from the discrete Fourier transform. (A gain of 0.5 with 100 iterations was used.) The power spectrum sampled over ~ -600 to -1100 km s^{-1} (i.e. the range of well-developed DACs) in P v is shown in Fig. 4. The data sampling are generally not intensive enough for a very robust period search, and the power in P v is spread across several frequencies. Nevertheless, we identify as potentially

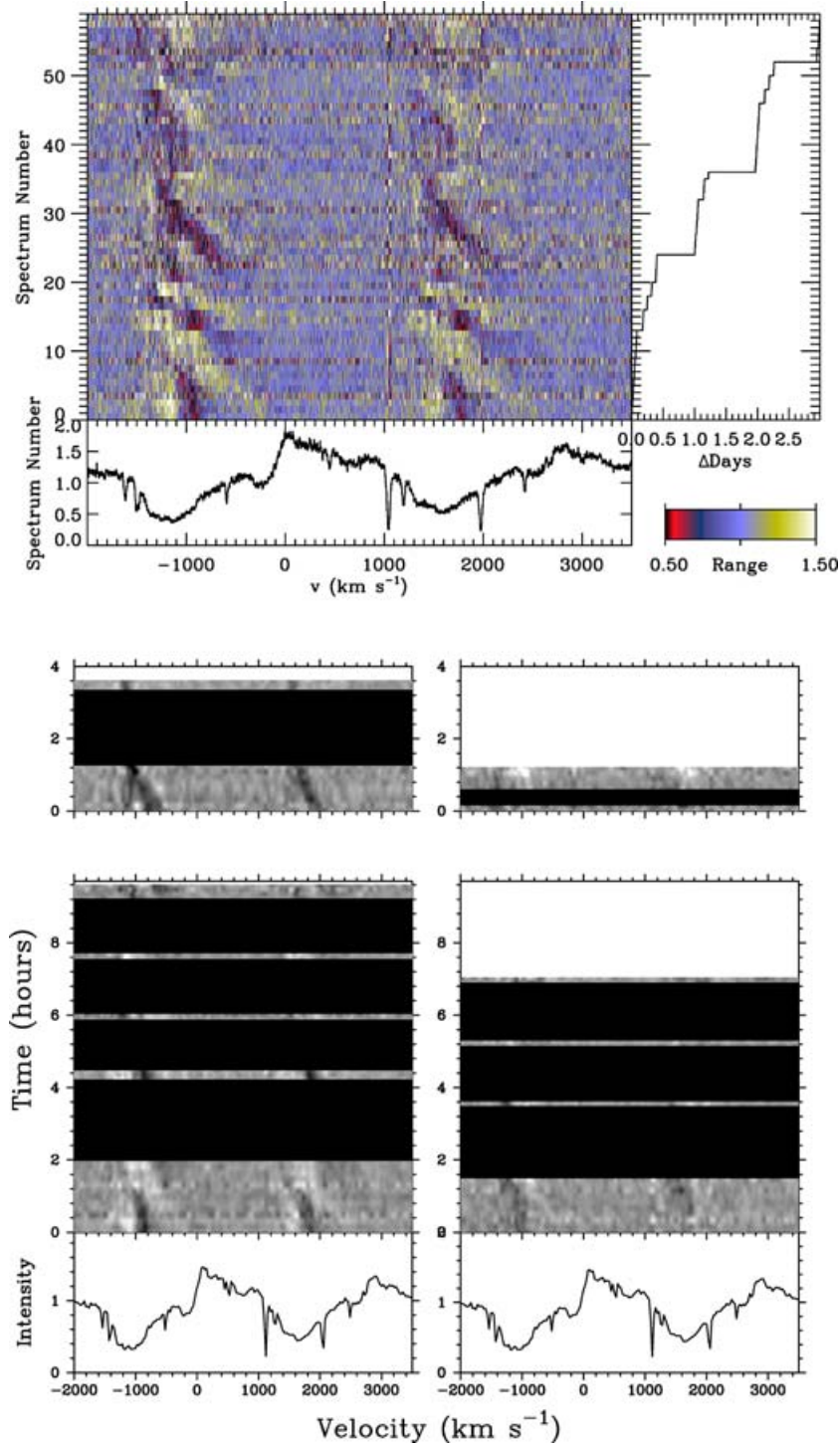


Figure 3. Dynamic spectrum representations of *organized*, hourly variability in P v $\lambda\lambda 1118, 1128$. In the upper plot, the ordinate is the sequential spectrum number and the right-hand panel is a temporal plot showing the relative time of each exposure. The greyscales in the lower plot show the *organized*, hourly variability. Starting from the bottom, data in the pair of (lower) left- and right-hand panels span a total of ~ 1.22 and 1.02 d, respectively. To enhance the contrast in these images, the individual spectra have been normalized by the mean profile for the time-series.

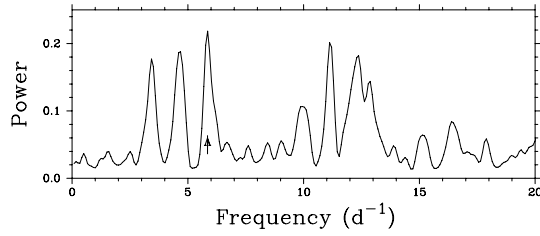


Figure 4. Power spectrum (in arbitrary units) for the P v *FUSE* time-series. The arrow marks the primary peak corresponding to a period of 0.17 d in P v (see Section 4).

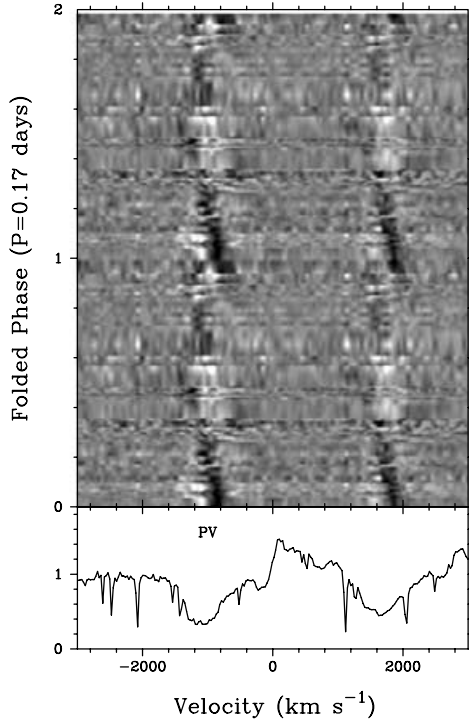


Figure 5. Individual P v spectra are shown phased over two cycles on a period of 0.17 d; a clearly coherent behaviour is evident.

interesting the main power peak in P v at $\sim 5.85 \text{ d}^{-1}$, corresponding to a period of $\sim 0.17 \text{ d}$. The half-width at half-maximum of the zeroth order peak in the window function provides an approximate (and conservative) estimate of the error in the frequency of $\sim 0.1 \text{ d}^{-1}$. Independent determinations of the period sampled over 300 km s^{-1} bins in the region between -600 and -1100 km s^{-1} suggest an error in the frequency of $\sim 0.5 \text{ d}^{-1}$. The adjacent peaks in the power spectrum (Fig. 4) are comparatively less stable in similar velocity bin sampling.

Greyscales of individual spectra normalized to the mean are shown in Fig. 5 phased on the 0.17 d period. The diagnostic P v data do clearly show some coherency on the 0.17 d time-scale. The modulation is represented by the occurrence of two sequential episodes of migrating structures in the wind. (Recall that the total length of the *FUSE* time-series combined here is $\sim 3 \text{ d}$, and therefore spans several ‘cycles’.)

Tentative evidence of variability on hourly time-scales can also be gleaned by examining *low-resolution* ($R \sim 300$) *IUE* spectra of the central star. We have retrieved from the European Space Agency *IUE* archive a sequence of 38 spectra (SWP54865 to SWP54960),

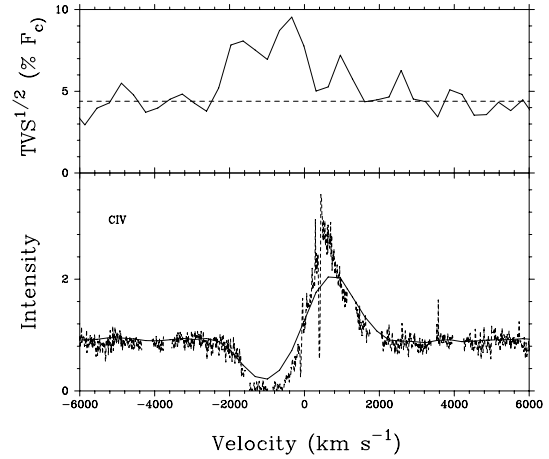


Figure 6. Variance spectrum for low-resolution *IUE* time-series of the C IV $\lambda\lambda 1548, 1550$ line in NGC 6543. The horizontal dashed line represents the 95 per cent confidence limit. The lower panel shows the low-resolution line profile (solid line) together with the a representative high-resolution *IUE* spectrum (dashed line).

which extend over 4.2 d. Despite being saturated, the blue wing of C IV is apparently highly variable (e.g. Patriarchi & Perinotto 1997). Furthermore, studies of fluctuations in the extended blue wings of saturated P Cygni profiles *have* (perhaps surprisingly) revealed evidence for modulated behaviour (see e.g. Howarth, Prinja & Massa 1995; Prinja et al. 1998). We used high-resolution *IUE* spectra of NGC 6543 that were degraded [by convolution with a 5 \AA full width at half-maximum (FWHM) Gaussian], to improve the internal consistency of the low-resolution data and to normalize the continuum fluxes near C IV. The variance characteristics of the low-resolution *IUE* C IV time-series are shown in Fig. 6. There is a double-peaked nature to the temporal variance spectrum (e.g. Fullerton, Gies & Bolton 1996), and we elect to sample, in particular, the profile changes between -1000 and -2000 km s^{-1} , since these are likely to represent variability in the extreme blue wings. However, no signal is detected in C IV at the frequency identified for P v modulations. The *IUE* data quality prevent us from making any firm conclusions as to whether any (quasi-)periodic signal in NGC 6543 is long-lived. We also attempted to phase-fold the original *photometric* data of Bell et al. (1994, obtained in 1993; Don Pollacco, private communication) but did not find any convincing evidence for a modulation on $\sim 0.17 \text{ d}$.

5 LINE-SYNTHESIS AND OPTICAL DEPTHS

In order to further quantify the physical properties of the DACs in the wind of NGC 6543, the *FUSE* resonance lines were modelled using the SEI method (see Lamers, Cerrutti-Sola & Perinotto 1987), with the modified procedures of Massa et al. (2003). The radial optical depth, $\tau_{\text{rad}}(w)$, is treated as 21 independent velocity bins (each $\sim 0.05 v_{\infty}$ wide) to provide greater flexibility in matching absorption optical depths in a structured wind that is affected by variable features such as DACs. We assume a standard parametrized velocity law of the form:

$$w = w_0 + (1 - w_0) \left(1 - \frac{1}{x} \right)^{\beta}, \quad (1)$$

where $w = v/v_{\infty}$ and $x = r/R_{\star}$. The effect of a photospheric spectrum in the SEI profile fitting is approximated by a Gaussian of

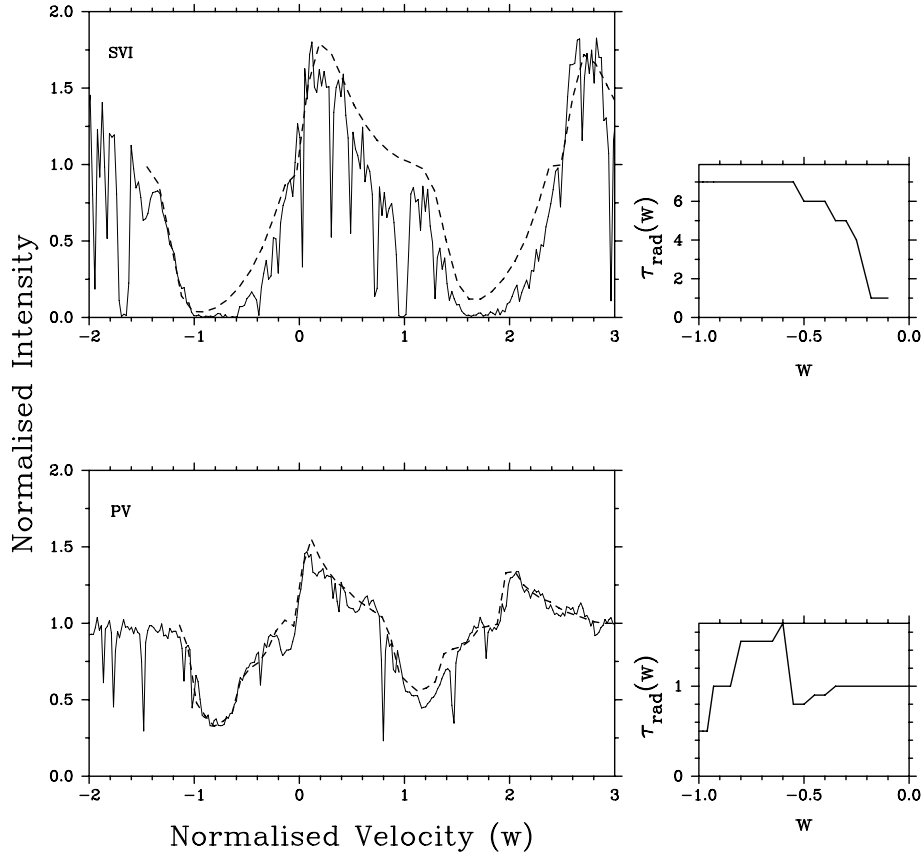


Figure 7. SEI model fits to the mean S VI $\lambda\lambda 933, 945$ and P V $\lambda\lambda 1118, 1128$. The adopted optical depth bins as a function of normalized velocity ($= v/v_\infty$) are shown in the right-hand panels.

FWHM = 250 km s^{-1} ; its effect is only to improve the match at low velocities ($\leq 0.2 v_\infty$) and does not impact seriously on the overall wind parameters derived in this section. Model fits to the mean P V profile in our time-series are shown in Fig. 7, where a very good overall match is achieved for $v_\infty = 1400 \text{ km s}^{-1}$, $\beta = 1$ and v_{turb} (the small-scale velocity dispersion parameter) = 0.05 . Note that the redward component of P V may be affected by the (neglected) contribution due to Si IV $\lambda\lambda 1122.5, 1128.3$. These values are also consistent for reproducing the blue wing of a much stronger (saturated) profile such as S VI (Fig. 7).

The central star is H-rich, with normal solar abundance ratios though Carbon may be overabundant (e.g. Georgiev et al. 2006). The SEI model of P V in Fig. 7 therefore gives a (mean) value for the product of mass-loss rate and ionization fraction, $\dot{M} q(P^{++})$, integrated over 0.2 to $0.9 v_\infty$, of $\sim 5.0 \times 10^{-9} M_\odot \text{ yr}^{-1}$ (for parameters in Table 1). Over the velocity range where the peak variance occurs in P V (i.e. ~ 0.5 to $0.9 v_\infty$), SEI fits to the cases of minimum and maximum observed absorption yield $\dot{M} q(P^{++})$ values of $\sim 1.9 \times 10^{-9}$ and $3.5 \times 10^{-9} M_\odot \text{ yr}^{-1}$.

The fact that the SEI model can match well the overall morphology of the observed absorption in P V permits us to model individual line profiles in the *FUSE* time-series. Specifically, we focus on the data covering the two most prominent DAC-like features in lower left-hand panels of Fig. 3 (in both the cases, the features start from the normalized time of 0.0 h ; the corresponding *FUSE* exposures are F03401050012 to F03401050082 and F03401060042 to F03401060122). The fits to these spectra, which are varying due to the occurrence of DACs, can then be compared with a ‘no-DAC’

case, that is, a spectrum representative of maximum flux over most velocities (i.e. F03401080072).

The SEI models fits to the P V (time-series) line profiles are shown in Fig. 8. The flexible optical depth bins are designed to allow matches to a wind profile that is obviously not ‘smooth’, but is instead distorted due to density, ionization or velocity features (see e.g. Massa et al. 2003). The good overall reproduction in Fig. 8 permits us to extract optical depths at the specific velocity of the migrating DACs and normalize them to the no-DAC case. Ratios of $\tau(\text{DAC})/\tau(\text{min})$ (obtained from fits to the individual profiles) are plotted as function of normalized velocity (v/v_∞) in Fig. 9. The plot therefore shows the optical depth evolution of two independent DAC episodes as a function of their central velocities. In both cases, the optical depth ratio due to DACs rises to a maximum of ~ 5 at $\sim 0.62 v_\infty$, and drops to ~ 2 towards $0.75 v_\infty$. The indication that the maximum contrast of the DACs is reached at intermediate velocities is somewhat unexpected. The increase in Sobolev optical depth at these positions may be due to a plateau in the wind velocity law, that is, a radially extended region of near-constant velocity. Wind material flows through the plateau, and the observed accelerations of DACs are then associated with the evolution (in velocity and radial extent) of the plateau as a function of time. The origin of such a plateau could, for example, relate to the formation of co-rotating interactions regions in the outflow (see e.g. Cranmer & Owocki 1996, and discussion in Section 6).

To gain some insights into the ionization balance and wind clumping in NGC 6543, we also employed the unified model atmosphere code CMFGEN (Hillier & Miller 1998), which calculates non-LTE

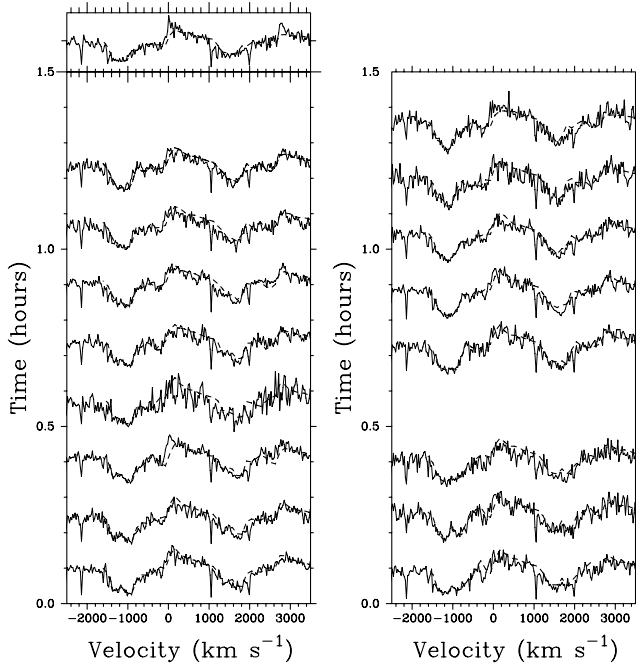


Figure 8. SEI model fits (dashed lines) to sequences of P v line profiles where two of the prominent DACs are migrating between ~ -600 and -1100 km s $^{-1}$, that is, the lower left-hand panels in Fig. 3. The isolated profile fitted in the upper left-hand panel is a representative ‘no-DAC’ (maximum flux) case.

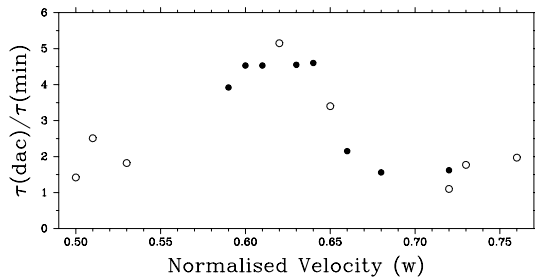


Figure 9. Ratio of optical depth in the DAC to minimum optical depth at that velocity from SEI fits, for two independent episodes (i.e. open and closed symbols) identified in Figs 3 and 8.

models of spherically symmetric winds with multilevel atoms. The fundamental parameters listed in Table 1 were adopted, together with $\log g = 4.2$ and a He/H abundance ratio (by number) of 0.1 (e.g. Georgiev et al. 2006). A parametric treatment of wind clumping is implemented in CMFGEN, in terms of the volume filling factor, f , defined as

$$f = f_{\infty} + (1 - f_{\infty}) \exp\left(-\frac{v}{v_{cl}}\right), \quad (2)$$

where v_{cl} is the velocity at which clumping starts, and which we adopt as 35 km s $^{-1}$ (i.e. above the sonic point). Our objective here is primarily to investigate the spectral signatures of clumping in CMFGEN models applied to the fast wind of NGC 6543, we do not attempt a detailed exercise in fitting several lines.

Models were run for cases of the clump volume filling factor, $f_{\infty} = 0.06, 0.08$ and 0.1 , and the synthesized spectra are compared in Fig. 10 to key wind lines in the *FUSE* and high-resolution *IUE* data of the central star. For a mass-loss rate of $6 \times 10^{-8} M_{\odot} \text{ yr}^{-1}$, the models

provide good overall fits to the observed resonance and excited state line profiles. It is interesting to note that the P v lines are particularly sensitive to the clumping factor, more so than O v and N iv. Our data favour the case of $f_{\infty} = 0.08$, though, of course, we neglect here the consequences of these parameters for reproducing diagnostic optical lines in the central star of NGC 6543, such as He II $\lambda 4686$ and C iv $\lambda 5801$. Fig. 11 displays the predicted ionization fractions of P $^{3+}$, P $^{4+}$ and P $^{5+}$ as a function of velocity and for the three different clumping factors. The dominance of P $^{5+}$ at low-velocities results in the mismatch with the observed profile seen in this region (Fig. 10). The ion fractions of P $^{3+}$ and P $^{4+}$ increase over all velocities for lower values of f_{∞} , with an increased recombination from P $^{5+}$ to P $^{4+}$ particularly evident at the highest velocities. The CMFGEN models run here generally predict C $^{4+}$ and P $^{5+}$ as dominant (i.e. $q_i > 0.97$ over ~ 0.2 to $0.9 v_{\infty}$), and S $^{5+}$ and O $^{4+}$ close to dominant (i.e. $q_i \sim 0.6$ and 0.2 , respectively).

Our results indicate that P v is a sensitive spectral diagnostic of *small-scale* clumping in the fast wind, together with the large-scale structures represented by the DACs discussed in Section 3. We highlight the need to adopt fairly small volume filling factors in order to match the P v resonance line doublet. P $^{4+}$ is a trace ion, just below dominant (Fig. 11), and is therefore extremely sensitive to changes as parametrized here, since its abundance depends strongly on density. This is in contrast to the results for O stars presented by Bourret et al. (2005), where P $^{4+}$ is dominant and not as sensitive to small fluctuations in density.

6 DISCUSSION

The empirical evidence presented here suggests that (i) the fast wind of NGC 6543 is highly variable on time-scales of hours, (ii) the wind changes are systematic in terms of recurrent absorptive optical depth structures that migrate blueward and (iii) the temporal behaviour of the P v resonance line P Cygni profiles is very similar to that due to the presence of DACs in luminous OB stars. A comparison between the DAC properties of NGC 6543 and a ‘representative’ mid-O giant is presented in Table 3, where the latter is summarized from various studies (see e.g. those cited in Section 3). We note that the fundamental characteristics such as initial detection at low Doppler velocities, recurrence, modulation and optical depth contrast are broadly similar for both cases; the same is also true for the (linear) acceleration scaled by the flow time-scale (R_{\star}/v_{∞}). There is some indication that the line-of-sight velocity dispersion of the DACs in NGC 6543 is somewhat smaller than for a typical O-type giant (such as ξ Per or 68 Cygni).

Our interpretation of these results therefore is that the physical mechanism responsible for the DAC structures in the fast wind of NGC 6543 is likely the same as that acting in massive OB stars. There remain several uncertainties in our understanding of this phenomena in massive stars, but in the particular case where quasi-periodic wind variability is detected, several authors have promoted a scenario in terms of co-rotating interaction regions (CIRs; e.g. Cranmer & Owocki 1996; Fullerton et al. 1997; de Jong et al. 2001). The notion is that the DACs are spectroscopic signatures of spatial structures in the wind that are causally connected to stellar surface irregularities. These photospheric inhomogeneities cause the wind from different longitudinal sectors on the stellar surface to emerge with different densities and/or velocities. The consequence is to form different adjacent streams that meet to create spiral-shaped CIRs. Key observational properties of the DACs can be matched with this model, with variable optical depth enhancements arising from the combination of a plateau in the radial velocity as well as

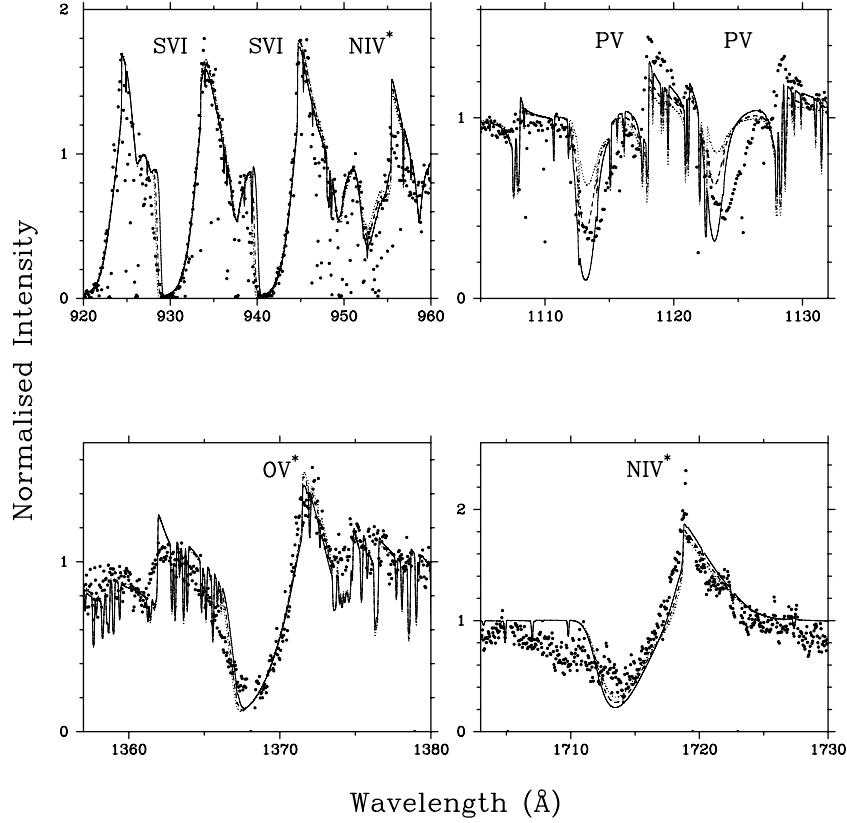


Figure 10. Key diagnostics lines in the *FUSE* and high-resolution *IUE* spectra (dots) of the central star are shown with CMFGEN model fits for $f_\infty = 0.06$ (solid line), 0.08 (dashed line) and 0.1 (dotted line). Notice the particular sensitivity of P V to the clumping factor.

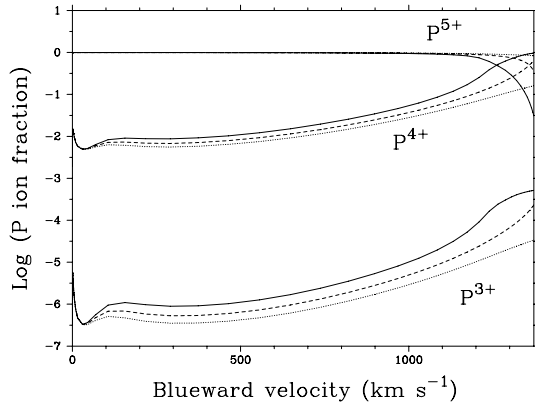


Figure 11. Log of the P IV, P V and P VI ion fractions as a function of blueward velocity, for cases of $f_\infty = 0.06$ (solid line), 0.08 (dashed line) and 0.1 (dotted line).

a density perturbation. In this model, the variations in absorption which occurs over significantly larger time-scales than the wind flow speed are due to gas flowing through a semipermanent, co-rotating structure. The rotation rate of the central star in NGC 6543 is unfortunately not known, and we are unable to comment further in this context on the significance of the ~ 0.17 -d period identified in Section 4. In the case of OB stars, the recurrence of DACs is mostly only quasi-cyclic, and has only rarely been demonstrated to be an integer relation to the stellar rotation rate. Nevertheless, our results provide the constraint that the mechanism for forming coherent perturbations in the outflows is apparently operating equally in the radiation-pressure-driven winds of widely differing momenta ($\dot{M}v_\infty R_*^{0.5}$) and flow times, as represented by OB stars and CSPN.

As regards the ‘trigger’ provided by photospheric irregularities for the growth of wind structure, the action of surface velocity fields due to pulsation and/or ordered magnetic fields may be just as applicable to CSPN as it is to OB stars. Multiperiod pulsation modes are thought to be the cause of short-period (approximately hourly)

Table 3. Comparison of NGC 6543 and mid-O star DAC properties.

DAC measure	NGC 6543	O stars (e.g. O7 III)
v_{initial}	$\sim 0.3 v_\infty$	$\leq 0.3 v_\infty$
Recurrence	Yes (over approximately hours)	Yes (over approximately days)
$(dv/dt)(R_*/v_\infty)$	$\sim 12\text{--}24 \text{ km s}^{-1}$	$\sim 10 \text{ km s}^{-1}$
Maximum $\tau(\text{DAC})/\tau(\text{min})$	~ 5	~ 5
Quasi-periodic	Yes; $P \sim 0.14 \text{ d}$	Yes; e.g. $P \sim \text{days}$
FWHM/v_∞ (initial)	$\sim 0.15 v_\infty$	$\sim 0.3 v_\infty$
FWHM/v_∞ (final)	$\leq 0.05 v_\infty$	$\leq 0.1 v_\infty$

variability seen in the photometric measurements of several central stars, including both H-rich and H-deficient cases (e.g. Ciardullo & Bond 1996; Handler et al. 1997). Kilogauss strength magnetic fields have also been detected (using spectropolarimetry) that are associated with the PN central stars (e.g. Jordan, Werner & O'Toole 2005), where they may be located mostly in the envelope, as opposed to the degenerate core, and can be affected by mass loss. One caveat here is that the link between pulsation or magnetic fields and repetitive wind structures in OB stars has thus far proved observationally very challenging and generally unconstrained; establishing such a connection in CSPN is going to be even more difficult!

The *ab initio* CMFGEN calculations presented in Section 5 favour a small clump volume filling factor, $f_\infty \sim 0.08$. Whether or not the parametrization of clumping incorporated in CMFGEN is physically meaningful, we note that the high sensitivity of the P V lines to the clumping factor is again similar to that apparent for the same line in O-type stars. Following the clumping studies of, for example Markova et al. (2004), Bouret et al. (2005), Fullerton et al. (2006), our results for NGC 6543 would imply a reduction by a factor of ~ 4 (i.e. $1/\sqrt{f_\infty}$) in the mass-loss rate due to the clumped fast wind compared to smooth-wind models. The analysis of *optical* lines with the non-LTE code FASTWIND by Kudritzki, Urbaneja & Puls (2006) also points to substantially clumped CSPN fast winds. Downward revisions in the central star mass-loss rate would affect the dynamics of the hot central cavity excavated by the fast wind, thus modifying its interaction with the surrounding nebula, including contributions to the X-ray emission. Naturally, our far-UV analyses need to be extended to cover a large sample of central stars to permit firm assessments of any revisions to CSPN mass-loss rates, and most importantly, tested for consistency between UV and optical diagnostics of clumping. Finally, looking ahead, the vastly increased sensitivity soon to be offered at radio wavebands by the upgraded e-MERLIN and EVLA facilities raises new possibilities for measuring the free-free emission from the fast wind itself, and thus provide a powerful new constraint on the central star mass loss.

ACKNOWLEDGMENTS

Based on the observations made with the NASA-CNES-CSA Far Ultraviolet Spectroscopic Explorer. *FUSE* is operated for NASA by the Johns Hopkins University under NASA contract NAS5-32985. DLM acknowledges support through NASA contract NNG07EF12P to SGT, Inc. SEH is grateful for studentship support from STFC (formerly PPARC).

REFERENCES

Akashi M., Soker N., Behar E., 2006, MNRAS, 368, 1706
 Balick B., 2004, AJ, 127, 2262
 Bell S. A., Pollacco D. L., Hilditch R. W., 1994, MNRAS, 267, 1053
 Bouret J.-C., Lanz T., Hillier D. J., 2005, A&A, 438, 301
 Chu Y.-H., Guerrero M. A., Gruendl R. A., Williams R. M., Kaler J. B., 2001, ApJ, 553, 55
 Ciardullo R., Bond H. E., 1996, AJ, 111, 2332
 Cranmer S. R., Owocki S. P., 1996, ApJ, 462, 469
 de Jong J. A. et al., 2001, A&A, 368, 601
 de Koter A., Hubeny I., Heap S. R., Lanz T., 1996, in Jeffery C. S., Heber U., eds, ASP Conf. Ser. Vol. 96, Hydrogen-Deficient Stars. Astron. Soc. Pac., San Francisco, p. 141

De Marco O., Bond H. E., Harmer D., Fleming A. J., 2004, ApJ, 602, 93
 Falle S. A. E. G., Coker R. F., Pittard J. M., Dyson J. E., Hartquist T. W., 2002, MNRAS, 329, 670
 Fullerton A. W., Gies D. R., Bolton C. T., 1996, ApJS, 103, 475
 Fullerton A. W., Massa D. L., Prinja R. K., Owocki S. P., Cranmer S. R., 1997, A&A, 327, 699
 Fullerton A. W., Massa D. L., Prinja R. K., 2006, ApJ, 637, 1025
 Georgiev L. N., Hillier D. J., Richer M. G., Arrieta A., 2006, in Barlow M. J., Mendez R. H., eds, IAU Symp. Vol. 234, Planetary Nebulae in Our Galaxy and Beyond. Cambridge Univ. Press, Cambridge, p. 119
 Guerrero M. A., Chu Y.-H., Gruendl R. A., Williams R. M., Kaler J. B., 2001, ApJ, 553, L55
 Handler G., 2003, in Sterken C., ed., ASP Conf. Ser. Vol. 292, Interplay of Periodic, Cyclic and Stochastic Variability in Selected Areas of the H-R Diagram. Astron. Soc. Pac., San Francisco, p. 183
 Handler G. et al., 1997, A&A, 320, 125
 Harrington J. P., Borkowski J., 1994, BAAS, 26, 1469
 Heap S. R., 1979, in Conti P. S., de Loore C. W. H., Reidel D., eds, IAU Symp. Vol. 83, Mass Loss and Evolution of O-type Stars. Reidel Publishing, Dordrecht, p. 99
 Hillier D. J., Miller D., 1998, ApJ, 496, 407
 Hillier D. J., Lanz T., Heap S. R., 2003, ApJ, 588, 1039
 Howarth I. D., Prinja R. K., Massa D. L., 1995, ApJ, 452, L65
 Jordan S., Werner K., O'Toole S. J., 2005, A&A, 432, 273
 Kaper L., Henrichs H. F., Nichols J. S., Snoek L. C., Volten H., Zwarthoed G. A. A., 1996, A&AS, 116, 257
 Kastner J. H., Balick B., Blackman E. G., Frank A., Soker N., Vrtelek D., Li J., 2003, ApJ, 591, 37
 Kudritzki R. P., Urbaneja M. A., Puls J., 2006, in Barlow M. J., Mendez R. H., eds, IAU Symp. 234, Planetary Nebulae in Our Galaxy and Beyond. Cambridge Univ. Press, Cambridge, p. 119
 Lamers H. J. G. L. M., Cerrutti-Sola M., Perinotto M., 1987, ApJ, 314, 726
 Maness H., Vrtelek S. D., 2003, PASP, 115, 1002
 Markova N., Puls J., Repolust T., Markov H., 2004, A&A, 413, 693
 Massa D. et al., 1995, ApJ, 452, L53
 Massa D., Fullerton A. W., Sonneborn G., Hutchings J. B., 2003, ApJ, 586, 996
 Mendez R. H., Herrero A., Machado A., 1990, A&A, 229, 152
 Moos H. W. et al., 2000, ApJ, 538, L1
 Patriarchi P., Perinotto M., 1997, A&AS, 126, 385
 Perinotto M., Cerrutti-Sola M., Benvenuti P., 1982, A&A, 108, 314
 Perinotto M., 1989, in Torres-Peimbert S., eds, IAU Symp. 131, Planetary Nebulae. Kluwer, Dordrecht, p. 292
 Prinja R. K., 1998, in Kaper L., Fullerton A. W., eds, ESO Astrophysics Symposia, Cyclical Variability in Stellar Winds. Springer-Verlag, Berlin, p. 92
 Prinja R. K., Massa D., Howarth I. D., Fullerton A. W., 1998, MNRAS, 301, 926
 Prinja R. K., Massa D., Fullerton A. W., 2002, A&A, 388, 587
 Reed D. S., Balick B., Hajian A. R., Klayton T. L., Giovanardi S., Casertano S., Panagia N., Terzain Y., 1999, AJ, 118, 2430
 Roberts D. H., Lehár J., Dreher J. W., 1987, AJ, 93, 968
 Sahnou D. J. et al., 2000, ApJ, 538, L73
 Sandquist E. L., Taam R. E., Chen X., Bodenheimer P., Burkert A., 1998, ApJ, 500, 909
 Schneider S. E., Terzian Y., Purgathofer A., Perinotto M., 1983, ApJS, 52, 399
 Steffen W., Lopez J. A., 2003, Rev. Mex. Astron. Astrofis., 15, 50
 Wesson R., Liu X.-W., 2004, MNRAS, 351, 935
 Zuckerman B., Aller L. H., 1986, ApJ, 301, 772
 Zweigle J. et al., 1997, A&A, 321, 891

This paper has been typeset from a $\text{\TeX}/\text{\LaTeX}$ file prepared by the author.